

# MULTIWAVELET PACKET IMAGE COMPRESSION: THEORY AND RESULTS

*Michael B. Martin*

Vision III Imaging  
1155 Herndon Parkway, Suite 200  
Herndon, VA 20170

*Amy E. Bell*

Dept. of ECE  
Virginia Tech  
Blacksburg, VA 24061-0111

## ABSTRACT

Advances in wavelet transforms and quantization methods have produced algorithms capable of surpassing the existing image compression standards like the Joint Photographic Experts Group (JPEG) algorithm. Even so, some images have high-frequency information that is not preserved well in standard wavelet-based compression algorithms. To this end, wavelet packets have been developed and have been shown to work well on these types of images, such as the famous Barbara image. Another transform, the relatively new multiwavelet transform, shows initial promise in surpassing the image compression capabilities of wavelets. Thus, it seems likely that a new technique called “multiwavelet packets” that combines the best features of both wavelet packets and multiwavelets would offer even better performance. This paper defines multiwavelet packets and presents experimental results demonstrating that multiwavelet packets can give performance comparable to, or in some cases superior to, the current wavelet packet techniques.

## 1. INTRODUCTION

Algorithms based on wavelets have been shown to work well in image compression. For some images, however, wavelet packets demonstrate a significant improvement in reconstructed image quality over the octave-band wavelet decomposition. This benefit comes from the ability of the wavelet packets to better represent high-frequency content, and high-frequency oscillating signals in particular. This allows wavelet packets to perform significantly better than wavelets for compression of images with a large amount of texture—such as the commonly used Barbara image. Experiments show that wavelet packet techniques applied to such images can outperform wavelet techniques [6, 14]. Researchers also point out that the perceived image quality is significantly improved using wavelet packets instead of wavelets, especially in the textured regions of the images. We will now consider a new approach

to improving wavelet packet-based image compression: multiwavelet packets.

Multiwavelets are a natural extension and generalization of wavelets. In theory, multiwavelets should perform even better than wavelets due to extra freedom in the design of multifilters. But previously published results still favor wavelets, since effective application of multiwavelets requires solving additional problems to those encountered with wavelets [9, 11]. Theoretical and experimental results in the study of multiwavelets have been steadily progressing, and all the key components for the application of multiwavelets to image compression are now in place. In particular, there now exist methods for construction of orthogonal and bi-orthogonal multifilters with desirable filter properties [13, 3], good preprocessing techniques [10, 11], and a method for symmetric signal extension for symmetric-antisymmetric (SA) multiwavelets [13].

This paper begins with an overview of the theory of wavelet packets and multiwavelets. The extension to multiwavelet packets is then presented, along with experimental results using recently-constructed orthogonal and biorthogonal SA multiwavelets. Finally, some comments about the effectiveness and limitations of the new techniques and suggestions for improved methods are given.

## 2. BACKGROUND

### 2.1. Wavelet Packets

The wavelet transform is one type of signal transform that may be used in image compression. But the wavelet transform often fails to accurately capture high-frequency information, especially at low bit rates where such information is lost in quantization noise. For many images with mostly “smooth” content, such as Lena, this is acceptable. But for images which contain large amounts of high-frequency detail, like Barbara, the perceived image quality loss can be severe. Hence another transform method must be employed. Coifman, Meyer, and

Wickerhauser developed such a technique based on the wavelet transform and called it wavelet packets [1].

A single level of a standard wavelet decomposition splits the input signal into lowpass and highpass coefficients

through filtering and downsampling. A multi-level wavelet filter bank involves iterating the lowpass-highpass filtering and downsampling procedure only on the output of the lowpass branch of the previous stage. Coifman et al. formulated an extension of the octave-band wavelet decomposition to a full tree decomposition by allowing the lowpass-highpass filtering and downsampling procedure to be iterated also on highpass (bandpass) branches in the tree [1]. They defined the new basis functions, called wavelet packets, as follows.

Let  $\phi(t)$  and  $\psi(t)$  be the scaling and wavelet functions, respectively, which obey the two-scale equations

$$\phi(t) = \sqrt{2} \sum_{k=-\infty}^{\infty} h_k \phi(2t-k), \quad (1)$$

$$\psi(t) = \sqrt{2} \sum_{k=-\infty}^{\infty} g_k \phi(2t-k). \quad (2)$$

Note that the sequences  $\{h_k\}$  and  $\{g_k\}$  are the scaling and wavelet filter coefficients. Now let  $u_0(t) \equiv \phi(t)$  and  $u_1(t) \equiv \psi(t)$ , and define

$$u_{2n}(t) = \sqrt{2} \sum_{k=-\infty}^{\infty} h_k u_n(2t-k), \quad (3)$$

$$u_{2n+1}(t) = \sqrt{2} \sum_{k=-\infty}^{\infty} g_k u_n(2t-k). \quad (4)$$

Taking dyadic rescalings and translations of these functions yields a library of functions  $\{2^{-j/2} u_n(2^{-j}t-k)\}$ . This library is overcomplete, but a proper complete basis can be found by selecting a subset of the library with the right set of parameters  $\{n, j, k\}$  [1].

The selection of a basis can also be viewed in terms of a tree structure, in which the set of elements of each basis corresponds in a one-to-one fashion to a particular set of terminal nodes of a binary tree. Some examples of possible basis selections are shown as trees in Figure 1. At each branching point in a tree, the upper branch is lowpass filtered and downsampled while the lower branch is highpass filtered and downsampled. For example, the tree in Figure 1a corresponds to the wavelet octave-band decomposition.

Wavelet packets impose increased computational complexity due to the need to select a basis. Selection of a “best” basis for any particular image may be performed in a number of ways. Coifman et al. suggest the use of an additive cost function that is applied to each set

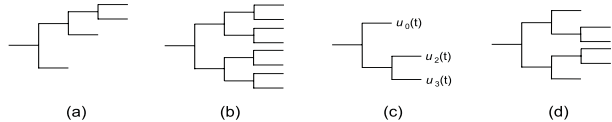


Figure 1: Possible wavelet packet filter banks. (a) is the standard wavelet decomposition, (b) is the full tree (Walsh basis), (c) and (d) are other possibilities.

of parent and child nodes in the pruning process. If the sum of the costs of the children is greater than the parent’s cost, the children are pruned; otherwise the children are kept. The performance of this method depends entirely on the choice of cost functions. Some cost functions that have been proposed include: Shannon entropy [2], the number of coefficients in the node that are significant compared to (i.e., greater than) some threshold<sup>1</sup> [6], and the number of bits required to represent all the coefficients in the node (introduced in this paper).

Newer methods for selecting a basis approach the problem from a rate-distortion perspective. Ramchandran and Vetterli proposed a method that attempts to select the set of terminal nodes that are optimal in a rate-distortion sense [7]. Their approach involves the minimization at each branch of a Lagrangian “cost function”,  $J(\lambda) = D + \lambda R$ , where  $D$  is the average distortion and  $R$  is the target average bit rate. The value of  $\lambda$  that minimizes  $J(\lambda)$  determines whether to prune and also gives the best quantizer for that node (which is then used for uniform quantization of the coefficients of that node). More recently, Xiong et al. have taken this idea and merged the basis optimization with their space-frequency quantization (SQF) approach, yielding impressive results [14].

## 2.2. Multiwavelets

A newer alternative to the wavelet transform is the multiwavelet transform. Multiwavelets are very similar to wavelets but have some important differences. In particular, whereas wavelets have an associated scaling function  $\phi(t)$  and wavelet function  $\psi(t)$ , multiwavelets have two or more scaling and wavelet functions. For notational convenience, the set of scaling functions can be written using the vector notation  $\Phi(t) \equiv [\phi_1(t) \phi_2(t) \cdots \phi_r(t)]^T$ , where  $\Phi(t)$  is called the multiscale function. Likewise, the multiwavelet function is defined from the set of wavelet functions as  $\Psi(t) \equiv [\psi_1(t) \psi_2(t) \cdots \psi_r(t)]^T$ . When  $r = 1$ ,  $\Psi(t)$  is called a *scalar* wavelet,

<sup>1</sup>Usually this threshold is taken to be on the order of the quantization step size.

or simply wavelet. While in principle  $r$  can be arbitrarily large, the best-studied multiwavelets so far have only  $r=2$ .

The multiwavelet two-scale equations resemble those for scalar wavelets:

$$\Phi(t) = \sqrt{2} \sum_{k=-\infty}^{\infty} H_k \Phi(2t-k), \quad (5)$$

$$\Psi(t) = \sqrt{2} \sum_{k=-\infty}^{\infty} G_k \Phi(2t-k). \quad (6)$$

Note, however, that  $\{H_k\}$  and  $\{G_k\}$  are *matrix* filters, i.e.  $H_k$  and  $G_k$  are  $r \times r$  matrices for each integer  $k$ . The matrix elements in these filters provide more degrees of freedom than a traditional scalar wavelet can possess. These extra degrees of freedom can be used to impart useful properties into the multiwavelet filters, such as orthogonality, symmetry, and high order of approximation.

### 3. NEW METHOD: COMBINING WAVELET PACKETS AND MULTIWAVELETS

#### 3.1. Multiwavelet Packets

Just as with scalar wavelets, the multiwavelet filter bank procedure involves iterating the filtering operation on the lowpass channel of the filter bank. And, just as with scalar wavelets, new basis functions can be produced by iterating on the highpass channels as well. This approach combines the wavelet packet decomposition with multiwavelet filters and hence we call it the multiwavelet packet decomposition. We define multiwavelet packets in a manner analogous to the wavelet packets in the last section.

Let  $U_0(t) \equiv \Phi(t)$  and  $U_1(t) \equiv \Psi(t)$ , and define

$$U_{2n}(t) = \sqrt{2} \sum_{k=-\infty}^{\infty} H_k U_n(2t-k), \quad (7)$$

$$U_{2n+1}(t) = \sqrt{2} \sum_{k=-\infty}^{\infty} G_k U_n(2t-k). \quad (8)$$

Note the similarity between (7) and (8) and the equivalent (3) and (4) from the last section. In fact, the tree structures representing bases for multiwavelet packets look just like those in Figure 1, with  $u_n(t)$  replaced by the corresponding vector-valued  $U_n(t)$ . For example, the wavelet packet tree in Figure 1 has a multiwavelet version that is shown in Figure 2.

The basis selection algorithms and cost functions used to prune the resulting tree structure are identical to those of the scalar wavelet packet case with

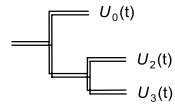


Figure 2: Possible multiwavelet packet filter bank. Compare to Figure 2(c).

one exception: the difference between wavelet packets and multiwavelet packets is that each branching in the tree structure creates four new channels (assuming  $r=2$ ) instead of just two, due to the dual-channel nature of multiwavelet filter banks. Since the multiwavelet packet tree then has four children for each parent, the computational complexity for multiwavelet packets may be higher than for wavelet packets. Cost function based methods will be essentially unaffected because they just operate on all the pixels corresponding to each node; with multiwavelet packets there are four nodes instead of two, but each node represents half as much data. However, methods that perform some form of rate-distortion optimization will require more computation due to the increased number of nodes.

#### 4. EXAMPLES AND FURTHER REMARKS

Image compression experiments were conducted for both scalar wavelet packets and the multiwavelet packets just described. Both orthogonal and biorthogonal multifilters were tested for multiwavelet packets, and all are from the class of symmetric-antisymmetric (SA) multifilters. The orthogonal SA multifilters used are “SA4” and “ORT4” [11, 13]; for biorthogonal SA multifilters we used “BSA7/5” and “BSA9/7” [3]. For comparison, two scalar wavelets were used for the wavelet packet tests: the popular biorthogonal “Bi9/7” filter and the recently presented “Bi22/14” biorthogonal filter [12].

Table 1 shows PSNR values for reconstructed images. Values shown in boldface represent the best result in each category. The number in parentheses following a filter name in Table 1 indicates which cost function was used for that case. Cost function “1” computes the cost as the number of significant coefficients<sup>2</sup> in the tested node. Cost function “2” computes the cost as the total number of bits required in the binary representation of all the coefficients in that node. All tests used the SPIHT quantizer [8] with no entropy coder. All multiwavelet packet tests use the preprocessing and signal extension method of Xia and Jiang [13] and the

<sup>2</sup>In this case, the threshold used for significance testing is simply 0.5, the threshold below which a coefficient will be converted to 0 during integer conversion.

decomposition iteration technique proposed by Martin and Bell [5]. The Barbara, Goldhill, and Mandrill images are the canonical 8bpp grayscale test images used frequently in the image compression literature. The “Testpat2” and “IC” images were taken from the MATLAB Image Processing Toolbox; these two images were chosen to represent “synthetic” image types in contrast to the “natural” character of the other images.

The results in Table 1 suggest multiwavelet packet performance on natural images is mixed. While the wavelet packets typically perform better at lower bit rates, multiwavelet packets give the best results at high bit rates on all but the Barbara image. For the Barbara image, the best wavelet packet result at each bit rate beat the best multiwavelet packet result by between 1.0 and 1.5 dB. However, for all the other images, even when one of the wavelet packets performs best at a given bit rate there is usually at least one multiwavelet packet result that comes close in PSNR. On the two synthetic images, multiwavelet packets give predominantly better results. In particular, the SA4 and BSA7/5 multiwavelet packets achieve perfect reconstruction (i.e. an MSE of zero) on the highly geometric Testpat2 image at 1.0 bpp. We also note that cost function “2” gives the best results in most cases. This is to be expected, as this cost function was chosen to work well with the SPIHT quantization method.

## 5. CONCLUSIONS

The multiwavelet packets used in this paper outperform wavelet packets on images containing large amounts of high-frequency content which is either mostly unstructured (as in Goldhill and Mandrill) or geometric or regular in nature (e.g. Testpat2 and IC). The only example in which wavelet packets gave better performance, Barbara, contains a large amount of structure to the coefficients in the subbands. The authors hypothesize that multiwavelet packets perform poorly in this case because the iterated multiwavelet transform produces a different subband structure than the wavelet transform. The structure assumed by SPIHT does not match the multiwavelet packet structure, and hence some performance is lost. The use of a different quantization method, such as a uniform scalar quantizer, should give better results for multiwavelet packets. Also, use of a rate-distortion optimization algorithm to select a multiwavelet packet basis should also improve results.

It should be pointed out that the scalar wavelets used here represent the best known filters published after years of study. In contrast, the multifilters used here are still quite new, and many have only been dis-

covered in the past year or so. It seems very likely that new multifilters will be published in the future which give even better performance than those in this paper. Even so, in many cases a multiwavelet packet can be selected which gives similar performance with lower computational complexity than the best scalar wavelet packet. This makes multiwavelet packets a viable alternative to scalar wavelet packets in many situations. Other new results for non-packet-based decompositions by Martin and Bell [5, 4] also confirm the good performance of multiwavelets applied to image compression.

## REFERENCES

- [1] R. R. Coifman, Y. Meyer, and M. V. Wickerhauser. Wavelet analysis and signal processing. In *Wavelets and their Applications*, pages 153–178. Jones and Bartlett, Boston MA, 1992.
- [2] R. R. Coifman and M. V. Wickerhauser. Entropy-based algorithms for best basis selection. *IEEE Trans. on Information Theory*, 38(2):713–718, March 1992.
- [3] Say Song Goh, Qingtang Jiang, and Tao Xia. Construction of biorthogonal multiwavelets using the lifting scheme. *preprint*, 1998.
- [4] Michael B. Martin and Amy E. Bell. New image compression techniques using multiwavelets and multiwavelet packets. *preprint*, 1999.
- [5] Michael B. Martin and Amy E. Bell. New methods and results in multiwavelet image compression. *preprint*, 1999.
- [6] F. G. Meyer, A. Z. Averbuch, and J. O. Strömberg. Fast adaptive wavelet packet image compression. *preprint*, 1998.
- [7] Kannan Ramchandran and Martin Vetterli. Best wavelet packet bases in a rate-distortion sense. *IEEE Trans. on Image Proc.*, 2(2):160–175, April 1993.
- [8] Amir Said and William A. Pearlman. A new, fast, and efficient image codec based on set partitioning in hierarchical trees. *IEEE Trans. on Circ. and Syst. for Video Tech.*, 6(3):243–250, June 1996.
- [9] V. Strela, P. N. Heller, G. Strang, P. Topiwala, and C. Heil. The application of multiwavelet filter banks to image processing. *preprint*, 1998.
- [10] V. Strela and A. T. Walden. Orthogonal and biorthogonal multiwavelets for signal denoising

and image compression. *Proc. SPIE*, 3391:96–107, 1998.

- [11] Jo Yew Tham, Li-Xin Shen, Seng Luan Lee, and Hwee Huat Tan. A general approach for analysis and application of discrete multiwavelet transforms. *preprint*, 1998.
- [12] Dong Wei, Hung-Ta Pai, and Alan C. Bovik. Anti-symmetric biorthogonal coiflets for image coding. *Proceedings of the IEEE International Conference on Image Processing (ICIP)*, October 1998.
- [13] Tao Xia and Qingtang Jiang. Optimal multifilter banks: Design, related symmetric extension transform and application to image compression. *preprint*, 1998.
- [14] Zixiang Xiong, Kannan Ramchandran, and Michael T. Orchard. Wavelet packet image coding using space-frequency quantization. *IEEE Trans. on Image Proc.*, 7(6):892–898, June 1998.

Table 1: PSNR results (in dB) for a few test images.

Image	Filter	1.000 bpp	0.500 bpp	0.250 bpp	0.125 bpp
Barbara	Bi9/7 (1)	35.02	30.67	27.37	24.89
	Bi9/7 (2)	35.84	31.30	27.83	25.18
	Bi22/14 (1)	35.71	31.23	27.85	25.21
	Bi22/14 (2)	<b>36.42</b>	<b>31.84</b>	<b>28.30</b>	<b>25.50</b>
	SA4 (1)	34.45	29.52	26.48	24.02
	SA4 (2)	34.34	29.62	26.75	24.37
	ORT4 (1)	34.50	29.59	26.54	24.08
	ORT4 (2)	34.45	29.68	26.78	24.41
	BSA9/7 (1)	33.67	29.26	26.38	24.35
	BSA9/7 (2)	34.61	30.02	26.78	24.24
Goldhill	BSA7/5 (1)	34.92	29.85	26.58	23.87
	BSA7/5 (2)	34.69	29.92	26.98	24.54
	Bi9/7 (1)	34.74	31.60	29.26	27.37
	Bi9/7 (2)	35.07	31.95	29.49	27.57
	Bi22/14 (1)	34.89	31.78	29.40	27.61
	Bi22/14 (2)	35.17	<b>32.01</b>	<b>29.52</b>	<b>27.75</b>
	SA4 (1)	34.88	31.58	29.02	27.13
	SA4 (2)	35.06	31.73	29.09	27.18
	ORT4 (1)	34.75	31.46	29.02	27.16
	ORT4 (2)	35.05	31.75	29.10	27.18
Mandrill	BSA9/7 (1)	34.13	31.25	28.99	27.16
	BSA9/7 (2)	34.84	31.65	29.25	27.58
	BSA7/5 (1)	34.94	31.64	29.11	27.21
	BSA7/5 (2)	<b>35.23</b>	31.82	29.16	27.27
	Bi9/7 (1)	26.97	23.98	21.96	20.95
	Bi9/7 (2)	27.53	24.37	22.23	<b>21.16</b>
	Bi22/14 (1)	27.08	24.08	22.06	20.97
	Bi22/14 (2)	27.73	<b>24.45</b>	<b>22.28</b>	21.14
	SA4 (1)	27.21	24.06	21.96	20.94
	SA4 (2)	27.76	24.36	22.21	21.04
Testpat2	ORT4 (1)	27.24	24.06	21.96	20.95
	ORT4 (2)	27.73	24.32	22.20	21.04
	BSA9/7 (1)	27.27	23.58	21.73	20.75
	BSA9/7 (2)	27.66	24.41	22.22	<b>21.16</b>
	BSA7/5 (1)	27.30	24.13	22.03	21.02
	BSA7/5 (2)	<b>27.84</b>	24.44	22.21	21.14
	Bi9/7 (1)	81.11	75.12	66.05	61.27
	Bi9/7 (2)	79.67	75.16	66.00	61.43
	Bi22/14 (1)	73.42	69.19	65.04	60.44
	Bi22/14 (2)	73.44	69.28	65.13	60.38
IC	SA4 (1)	$\infty$	78.23	70.51	63.42
	SA4 (2)	$\infty$	78.44	70.60	63.42
	ORT4 (1)	96.30	77.97	70.66	<b>63.46</b>
	ORT4 (2)	96.30	77.54	70.81	<b>63.46</b>
	BSA9/7 (1)	87.84	79.86	70.52	62.32
	BSA9/7 (2)	87.84	80.73	70.98	62.69
	BSA7/5 (1)	$\infty$	<b>82.32</b>	70.67	62.86
	BSA7/5 (2)	$\infty$	81.82	<b>71.12</b>	62.86
	Bi9/7 (1)	34.01	29.82	25.83	22.21
	Bi9/7 (2)	35.09	30.55	26.10	22.29
IC	Bi22/14 (1)	34.28	29.91	26.07	<b>22.36</b>
	Bi22/14 (2)	35.01	30.43	25.94	21.80
	SA4 (1)	34.64	29.97	25.55	21.61
	SA4 (2)	35.47	30.89	26.01	21.63
	ORT4 (1)	34.65	29.99	25.62	21.67
	ORT4 (2)	35.48	30.93	26.06	21.72
	BSA9/7 (1)	33.31	29.49	25.91	22.08
	BSA9/7 (2)	34.86	30.28	26.07	22.25
	BSA7/5 (1)	34.72	29.78	25.74	22.20
	BSA7/5 (2)	<b>35.72</b>	<b>30.95</b>	<b>26.37</b>	21.89